Asian Journal of Chemistry; Vol. 35, No. 7 (2023), 1659-1664

ASIAN JOURNAL OF CHEMISTRY

https://doi.org/10.14233/ajchem.2023.27949

Synthesis of Tartaric Acid based Polymer Nanocomposite Incorporated with Copper Oxide Nanoparticles with Antibacterial Activity

K. SUBASHINI[1,2], V. SUJATHA[2,3,*] and S. PRAKASH[2,4]

[1]Department of Chemistry, Applied Sciences, New Horizon College of Engineering, Bangalore-560103, India
[2]Department of Chemistry, Periyar University, Salem-636011, India
[3]Present address: DST-Mobility Fellow, Department of Chemistry, Pondicherry University, Puducherry-605014, India
[4]P.G. Department of Chemistry, Vivekanandha Arts and Science College for Women, Sankari-637303, India

*Corresponding author: E-mail: chemsujatha888@gmail.com

Received: 30 April 2023; *Accepted*: 26 May 2023; *Published online*: 6 July 2023; AJC-21288

The copper oxide nanoparticles were synthesized using *Brassaia actinophylla* (*B. actinophylla*) flower extract by solution combustion method. The poly(tartaric acid-*co*-diethylene glycol-*co*-acrylic acid (TDA) hydrogel was prepared using tartaric acid (T), diethylene glycol (D) and acrylic acid (A). The synthesized CuO nanoparticles were introduced into TDA hydrogel and the polymer nanocomposite TDA-CuO was obtained. The UV-peak was observed at 270 nm for TDA-CuO nanocomposite and for TDA no peak found. Fourier transform infrared (FT-IR) peak obtained at 432 cm^{-1} confirmed the presence of CuO nanoparticles in the hydrogel. The nanoparticles size 25-35 nm was confirmed by transmission electron microscope (TEM) and the morphology was examined by scanning electron microscopy (SEM) analysis. The percentage of copper and oxygen was analyzed by energy dispersive X-ray analysis (EDAX) spectrum where the percentage of copper is 2.4%. The thermal stability of TDA and TDA-CuO hydrogel was confirmed by thermogravimetric analysis (TGA). The antibacterial activity was performed against two Gram-positive *Staphylococcus aureus* and *Bacillus subtilis* and two Gram-negative *Escherichia coli*, *Klebsiella pneumonia* bacterial strains at various concentrations 25, 50, 75 and 100 µL by agar well diffusion method. The Gram-positive bacterial strains showed highest antibacterial activity than Gram-negative bacterial strain at highest concentration 100 µg/mL.

Keywords: Nanoparticles, Hydrogel, Polymer composite, Antibacterial activity.

INTRODUCTION

Metal oxide nanoparticles are utilized in various fields such as material chemistry, medicine field, agriculture sector, information and technology, due to their exclusive properties like smaller size, high surface-area-to-volume proportion, surface modifiability and incredible biocompatibility. Metal oxides like ZnO, TiO_2 and SnO_2 used as an biosensor to detect cancer cells, these metal oxides enters easily into cancer cells, interact with the cancer tumor cells and eradicates cancerous tumors [1]. Metal oxides derived from plant extracts shows various biological activity. Example green synthesized CuO nanoparticles using *Aloe vera* leaf extract acts as an effective antibacterial activity against fish bacterial pathogens [2]. *Brassaia actinophylla* also called as *Schefflera actinophylla* and contains several phenolic and flavonoid compounds, which shows antioxidant and antimicrobial activities [3,4].

Tartaric acid is an organic acid, available naturally in many fruits (it is obtained as a byproduct during wine extraction from grapes), easy accessible and cheap. Over consumption of tartaric acid leads to vomiting, diarrhea, abdominal pain. It is an effective complexing agent, due to the presence of two hydroxyl and two carboxyl groups nanomaterial synthesis can be carried out with controllable morphology [5,6]. Tartaric acid is a crosslinking and chelating agent interacts with the hydroxyl group of other monomers, which prevents the metal ion aggregation [7]. Tartaric acid incorporated poly(N-vinyl 2-pyrrolidone-*g*-tartaric acid) hydrogels used to remove uranyl ions present in the waste water [8].

Diol is an organic compound, miscible with water, colourless liquid, easily biodegrade in soil and water. The flexibility and biocompatibility of hydrogels can be improved by using bi-functional monomers such as diethylene glycol. Diethylene

glycol based hydrogel increases pH sensitive and swelling behaviour of hydrogel. In ICD (indole-3-acetic acid (I), citric acid (C) and diethylene glycol (D)) hydrogel one of the monomer used is diethylene glycol, this hydrogel showed effective anti-fungal activity against *Aspergilus fumigates*, *Candida albicana* and *Rhizopus oryzae* [9].

These are ester derivatives, used as an important raw material in the synthesis of polymeric materials. Polymers developed using acrylic acid have good elasticity, stability to light and heat resistance. Mainly it is produced by petrochemical industries using crude oil as a raw material. Acrylic acid is synthesized using lactic acid by catalytic dehydration [10].

Acrylic acid is insoluble in aqueous medium at low pH. The hydrophilicity and wrinkle recovery of some textile surfaces has been improved by acrylic acid. Acrylic acid used in super absorbant polymers (SAPs) with highest water absorption band of 129-2300 g/g. Poly(acrylic acid) (PAA) are used to prevent the scale formation in the desalination process [11]. Acrylic acid polymers cover very huge range of applications such as cosmetics, varnishes, textiles, plastics, synthetic resins, synthetic rubber and lattices [12-15].

EXPERIMENTAL

The chemicals *viz*. copper nitrate, tartaric acid, acrylic acid, diol were purchased from Sigma Aldrich (Bangalore, India) and used as such.

Preparation of plant extract: *Brassaia actinophylla* belongs to Araliaceae family flowers were collected from the local garden of Bangalore city, India. The flowers were washed with distilled water and dried inside the room to avoid sunlight and made into powder using mixer grinder and sieved and the powder was taken into Soxhlet apparatus mixed with de-ionized water and the temperature was maintained between 50-60 ºC and the extraction process was carried out for 68 h. The plant extract was made concentrated using rotary flash evaporator, then dried in hot air oven, the dried nanoparticles were stored in air tight container for further use.

Synthesis of TDA hydrogel: The hydrogel poly(tartaric acid-co-diethylene glycol-co-acrylic acid (TDA) was synthesized using three different monomers, tartaric acid (T), diethylene glycol (D) and acrylic acid (A). At the beginning TD-pre-polymer was prepared using tartaric acid and diethylene glycol with the removal of water molecule by condensation polymerization. The third monomer acrylic acid was added with TD pre-polymer, again water molecule was removed, finally TDA hyrdrogel was synthesized, no crosslinkers were used in the process. Various steps involved in the synthesis process are shown in **Scheme-I**.

Synthesis of TDA-CuO nanocomposite: During the synthesis of TDA-CuO polymer nanocomposite, 0.2 g of green synthesized nanoparticles obtained from *B. actinophylla* flower extract were added into TDA hydrogel with constant stirring at 160 ºC for 4 h. Polymer nanocomposites TDA-CuO was obtained by fabricating CuO nanoparticles in to TDA hydrogel, it appeared in black colour.

RESULTS AND DISCUSSION

NMR studies: The structure of TDA hydrogel has been confirmed by ^{1}H NMR and ^{13}C NMR analysis. In ^{1}H NMR spectrum of TDA hydrogel (Fig. 1a), the small peaks appeared at δ_H (ppm) 6.1, 6.2 value indicates protons of (=CH_2) terminal acrylate structure and the peak at 4.31 shows proton peaks of (CH(OH)COOH) group of tartaric acid [16]. Peaks between 3.48 to 4.5 ppm confirms protons present in (O-CH_2-CH_2-O-) moiety in the TDA network, also 4.4 ppm is OH group of and 3.62 ppm is protons of (–CH_2) group of diethylene glycol [17].

Carbon chemical shift ^{13}C of TDA hydrogel is shown in Fig. 1b, the δ_C (ppm) peak value at 40.5 ppm (–CH_2– and –CH– carbon peaks in hydrogel network) indicates the corner CH_2 group of acrylic acid [18,19]. The signals δ 60-65 ppm due to carbon in polyester network –CO-O-CH_2-CH_2–, carbon atom of OH bearing tartaric acid is observed at δ 72.6 ppm, carbon atom of diethylene glycol at δ 72.8 ppm [20]. Acrylic acid carbon peak appeared at δ 128.9 and 132.2 ppm. Tartaric acid carbon peak at 173.5 ppm and peaks between 167.4 to 172.0 ppm is carbonyl atom of ester and acid in polyester chain [20]. The ^{1}H and ^{13}C NMR analysis confirmed the presence of all three monomers in the synthesized TDA hydrogel, further UV-visible and FT-IR reports support the NMR report.

UV-visible studies: The UV-visible spectrum of TDA hydrogel is shown in Fig. 2a. The pure form of TDA hydrogel did not show any peak; similarly no peaks were observed for pure form of starch reported by [21]. The CuO nanoparticles introduced polymer nanocomposite TDA-CuO peak was identified at 270 nm (Fig. 2b), but for the CuO nanoparticles UV-peak was identified at 277 nm. The UV absorption value of CuO

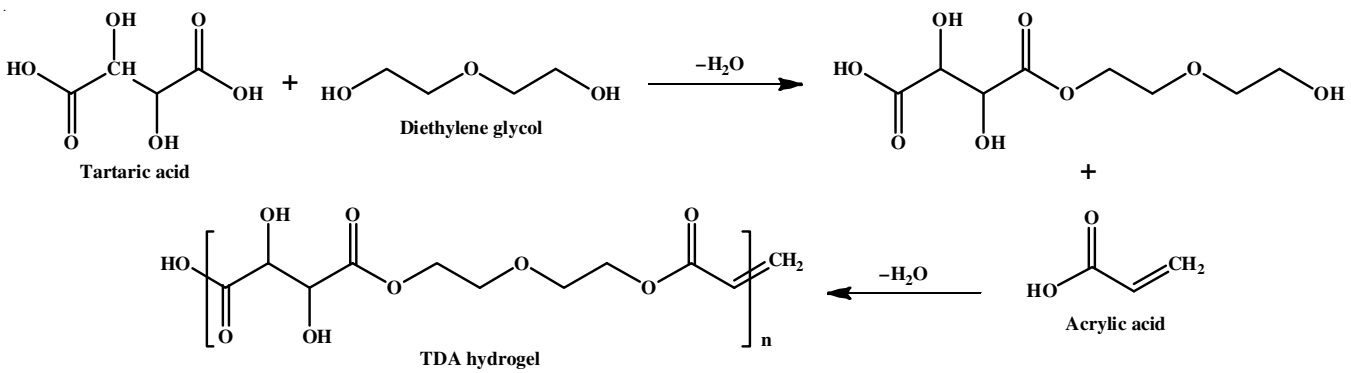

Scheme-I: Synthesis of TDA hydrogel

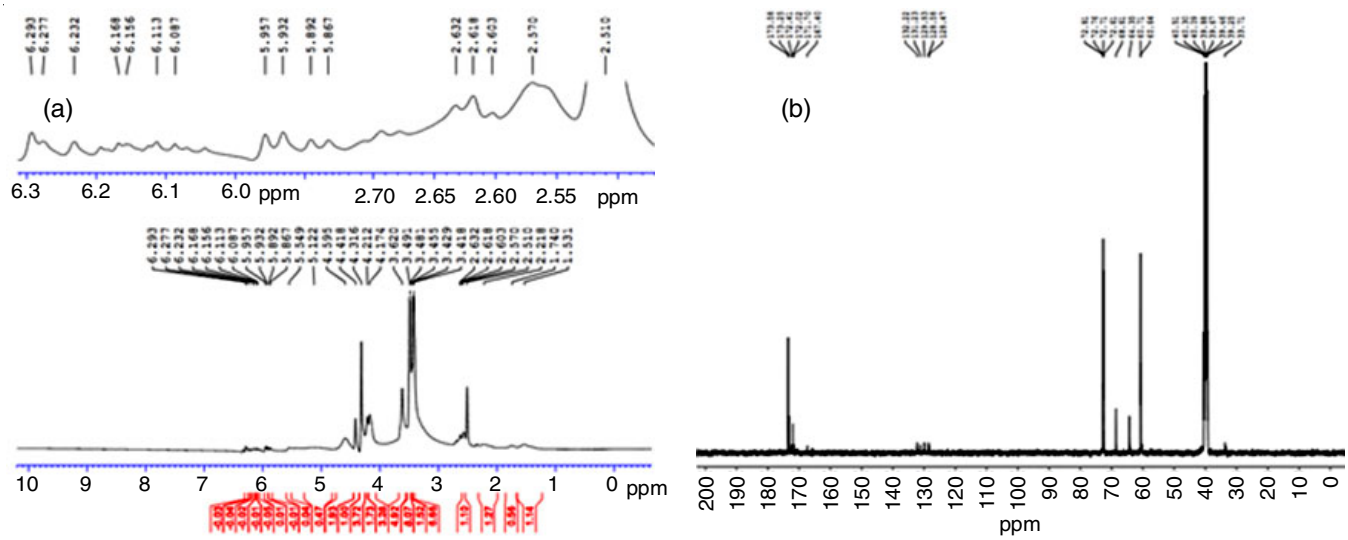

Fig. 1. ^{1}H NMR of TDA hydrogel (a), ^{13}C NMR of TDA hydrogel (b)

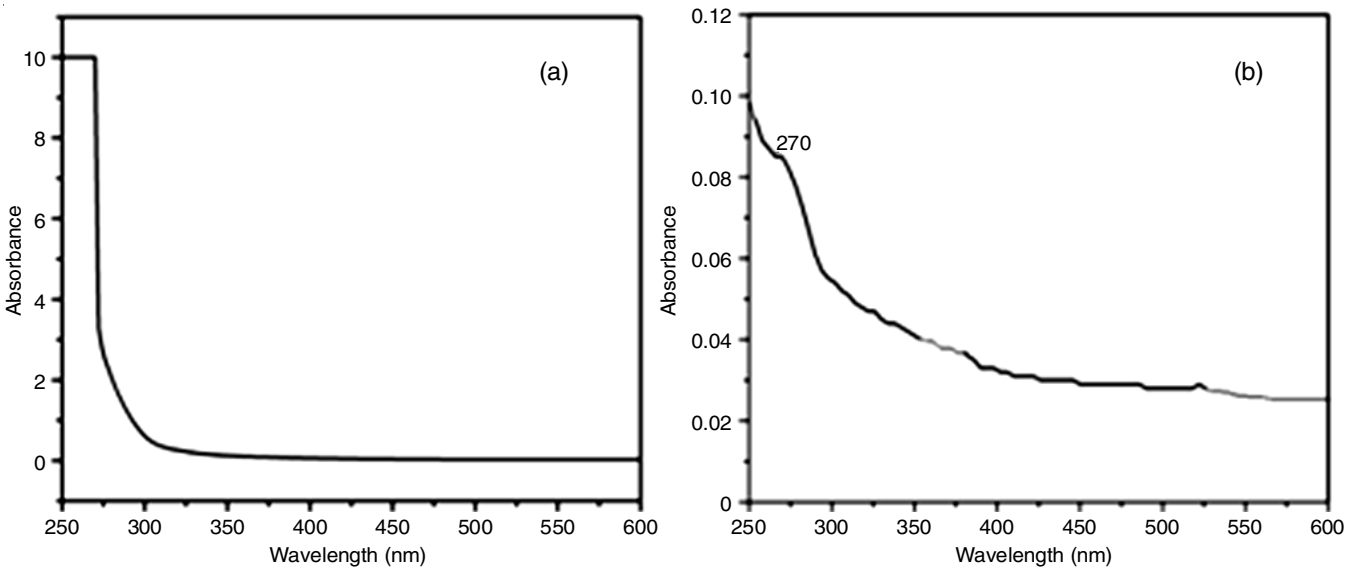

Fig. 2. UV-Vis spectrum TDA hydrogel (a), polymer nanocomposites TDA-CuO (b)

nanoparticles was reduced after introducing into TDA hydrogel due to surface plasmon resonance effect of CuO nanoparticles. The nanoparticles bound to the hydrogels and decreased the light scattering; this may be the another reason for reduced absorption peak of TDA-CuO hydrogel [22].

FT-IR studies: The FT-IR peaks of TDA and TDA-CuO are shown in Fig. 3. Presence of tartaric acid was confirmed by symmetric stretching vibration peak of OH group obtained at 3425 cm^{-1} [23. The acrylate unit –CH stretching peak was obtained at 2945 cm^{-1} [24], while the acrylic acid ester bond peak was appeared at 1735 cm^{-1} [25]. Tartaric acid COO– group asymmetric stretching vibration found at 1632 cm^{-1} [23]. The –CH_2– stretching vibration of polymer chain was observed at 1410 cm^{-1} [26]. The C-H group bending vibration observed at 1281 cm^{-1} [27]. The peak at 1126 cm^{-1} due to –C-O stretching bond of diethylene glycol [28]. The polymer epoxide link observed at 1066 cm^{-1} [24]. The bending and stretching vibration of CuO nanoparticles were identified at 680 cm^{-1} [29]. The CuO NPs binding in polymer chain peak obtained at 432 cm^{-1} [30].

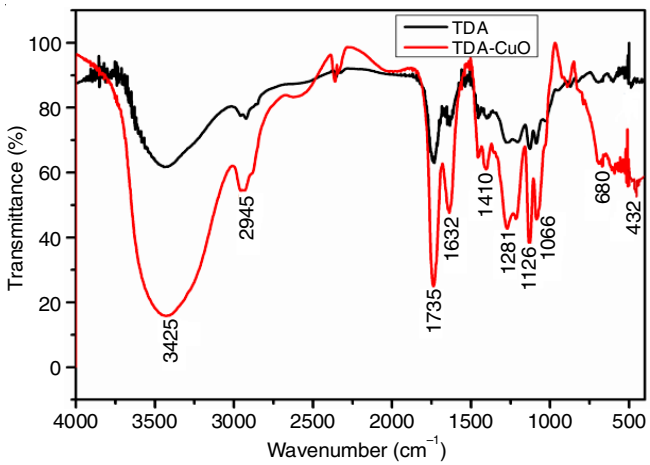

Fig. 3. FT-IR peak of TDA hydrogel and polymer nanocomposites TDA-CuO

SEM analysis: The morphology of TDA hydrogel and polymer nanocomposites are observed through SEM images.

The wrinkled and unequal pores found in the surface of TDA hydrogel (Fig. 4a-b). The pores present in TDA hydrogel improves the water intake of hydrogel, so that it becomes biocompatible in nature, similar image was observed for the chitosan [19]. The CuO nanoparticles was uniformly spread in the TDA hydrogel as shown in Fig. 4c-d, atomic percentage of CuO nanoparticles was maintained properly during polymer nanocomposite formation; same method was followed in earlier study for PVA/CuO matrix synthesis [31].

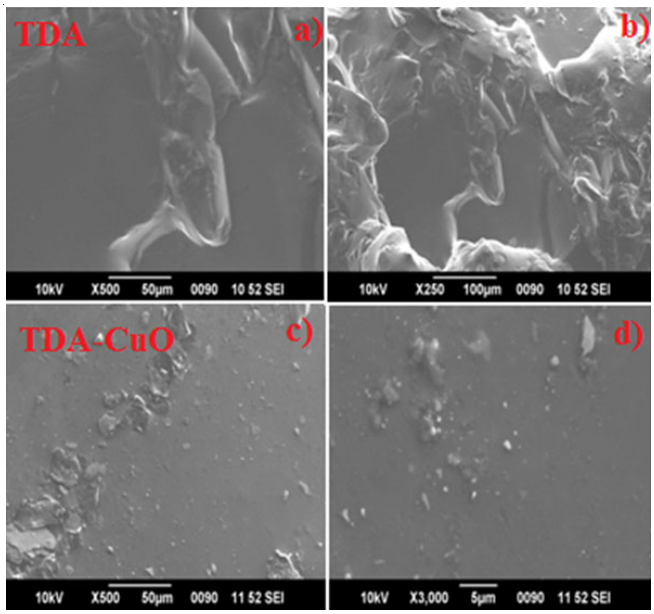

Fig. 4. SEM images of TDA hydrogel (a,b), Polymer nanocomposite TDA-CuO (c,d)

EDX studies: The elements present in the hydrogel TDA and polymer nanocomposites were identified using energy dispersive X-ray analysis graph. Atomic percentage of carbon 43.57% and oxygen 56.43% are shown in the TDA hydrogel (Fig. 5a). The atomic percentage of elements present in the TDA-CuO polymer nanocompoiste are carbon 47.32%, oxygen 49.4%, copper 2.4% and silicon 0.88% (Fig. 5b).

TEM studies: The morphology and size of the metal oxide nanoparticles present in the TDA-CuO, TDA-ZnO and TDA-NiO polymer nanocomposites were measured through TEM analysis. The average size of CuO nanoparticles embedded on the surface of TDA hydrogel were 25 to 35 nm and the CuO nanoparticles were dispersed on the entire surface of the polymer nanocomposite, so that there were more changes of improved biological activity of TDA-CuO polymer nanocomposite than the other polymer nanocomposites (Fig. 6a-d). The dispersion CuO nanoparticles were good than other metal oxides. Similar observation was made in cellulose nanocrystals, where CuO nanoparticles of average size 7 nm added into cellulose to synthesize cellulose/CuO nanocomposite and it was recommended for catalysis, sensor and various other applications [32]. Same applications can be implemented in TDA-CuO polymer nanocomposite and can be used for various biomedical applications.

Thermogravimetric analysis (TGA): The TGA analysis curve reveals the thermal stability of hydrogel and polymer nanocomposites. The TDA hydrogel curve observed with initial weight loss 20% from 0 to 100 ºC due to water evaporation and 20% weight loss between 100 to 250 ºC for the degradation of TDA hydrogel and second stage degradation was continued to 50% weight loss from 250 to 300 ºC. There is no specific weight loss noticed between 300 to 450 ºC (Fig. 7a). The

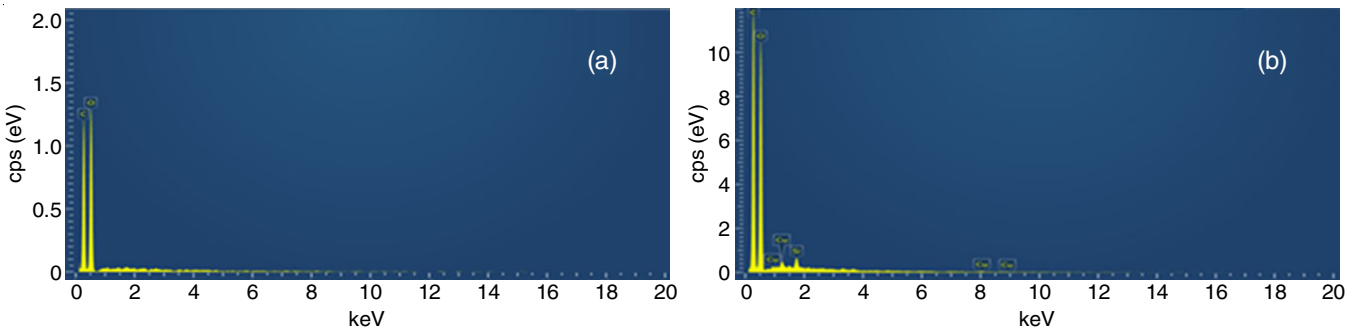

Fig. 5. EDAX spectrum of TDA hydrogel (a), polymer nanocomposite TDA-CuO (b)

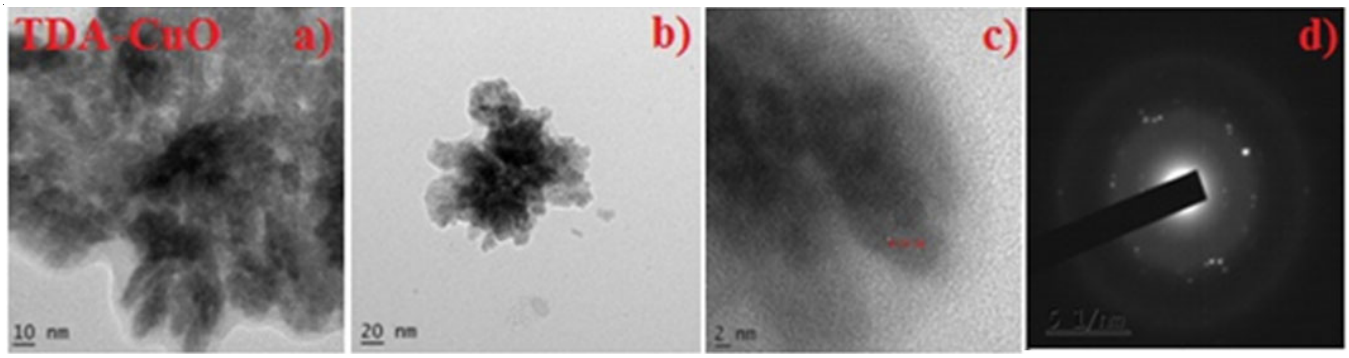

Fig. 6. TEM images of polymer nanocomposites TDA-CuO (a,b,c), SAED pattern of TDA-CuO (d)

hydrogel TDA was degraded within 450 ºC but the CuO nanoparticles incorporated polymer nanocomposite TDA-CuO thermal stability was extended up to 800 ºC (Fig. 7b) [31]. From the TGA results, it has been concluded that the thermal stability TDA-CuO polmer nanocomposite was higher than the other nanocomposites.

Antibacterial activity: Antibacterial activity of polymer nanocomposite TDA-CuO and TDA hydrogel was tested against two Gram-positive *Staphylococcus aureus* and *Bacillus subtilis* and two Gram-negative *Escherichia coli*, *Klebsiella pneumonia* bacterial strains at various concentrations 25, 50, 75 and 100 µL by agar well diffusion method and the zone of inhibition values are given in Table-1.

The zone of inhibition values against Gram-positive and Gram-negative bacterial strains are less at the higher concentration 100 µg/mL for pure hydrogel TDA when compared to polymer nanocomposites. The antibacterial activity of hydrogel has been increased by the addition of nanoparticles. The pure form of CMC (carboxymethyl cellulose) showed poor activity like TDA hydrogel [33]. The CuO nanoparticles embedded TDA-CuO polymer nanocomposite showed improved antibacterial activity, for Gram-positive bacteria *S. aureus* (38 mm), *B. subtilis* (37 mm) and Gram-negative bacteria *E. coli* (25 mm), *K. pneumoniae* (41 mm) for 100 µg/mL. The zone of inhibition observed for TDA-CuO against *K. pneumoniae* strain was higher than other strains, because the Gram-negative bacteria has thin peptidoglycan layer which is of 2 to 3 nm, at the same time for Gram-positive bacteria external layer composed of phospholipids and proteins are of nearly 30 nm, so CuO nanoparticles present in TDA hydrogel gets attached on the cell wall of bacteria and develops pores on its external surface and causes the protein leakage, further it continuous and causes to bacterial cell death [34].

Conclusion

The poly(tartaric acid-*co*-diethylene glycol-*co*-acrylic acid (TDA) hydrogel was prepared using T-tartaric acid, D-diethylene glycol and A-acrylic acid. The TDA-CuO polymer nanocomposites were prepared by adding green synthesized CuO nanoparticles into TDA hydrogel. Various characterizations like UV, FT-IR, XRD, FE-SEM, TEM and TGA were performed for the polymer nanocomposites to confirm the size and morphology of the NPs. From the results of TGA analysis, TDA-CuO polymer nanocomposite found to be thermally more stable. The antibacterial activity of *K. pneumoniae* bacterial strain was higher than other strains for the synthesized polymer nanocomposites. Particularly, TDA-CuO exhibited with higher antibacterial activity than TDA hydrogel.

CONFLICT OF INTEREST

The authors declare that there is no conflict of interests regarding the publication of this article.

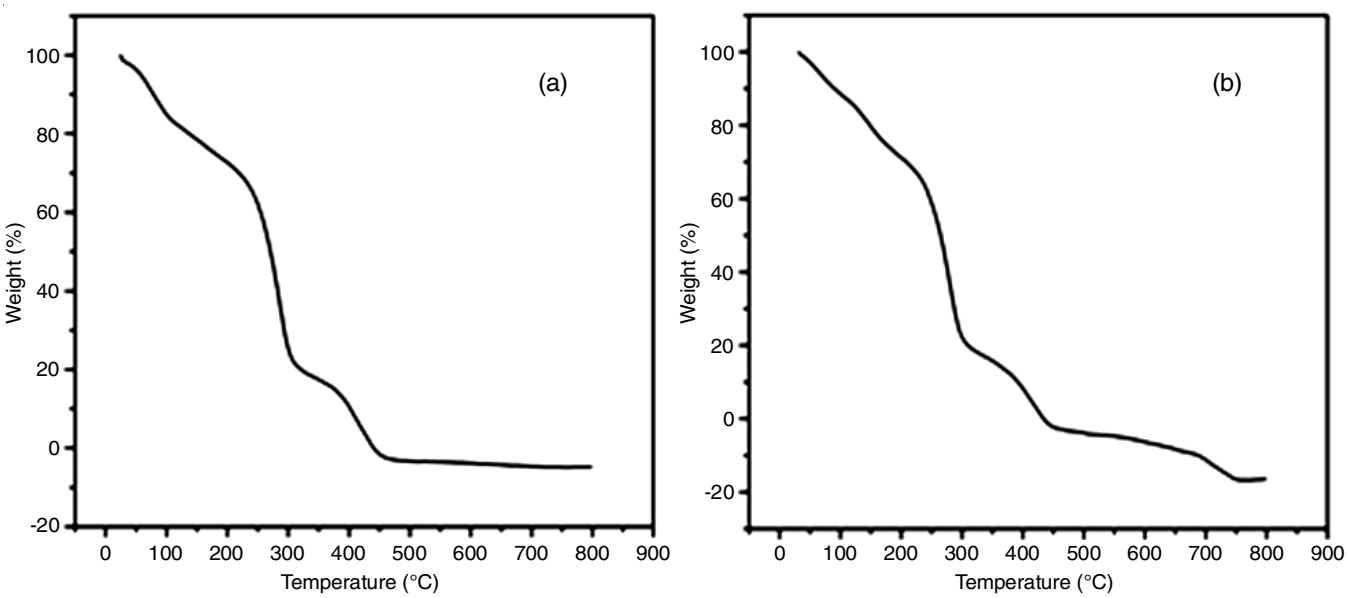

Fig. 7. Thermogravimetric curves of hydrogel TDA (a) and polymer nanocomposites TDA-CuO (b)

TABLE-1
ZONE OF INHIBITION VALUES OF TDA HYDROGEL, TDA-CuO

Organisms	Zone of inhibition (mm)									
	Various concentration of TDA (µL)					Various concentration of TDA-CuO NCs (µL)				
	25	50	75	100	*C	25	50	75	100	*C
S. aureus	12	15	19	21	35	21	33	36	38	35
B. subtilis	11	14	20	21	39	32	23	34	35	37
E. coli	9	12	18	19	37	21	22	24	25	36
K. pneumoniae	11	13	15	18	45	27	34	40	41	43

*C is control standard antibiotic drug Ciprofloxacin (75 µL). (Ciprofloxacin) positive control and (DMSO) negative control.

REFERENCES

1. D. Frank, C. Tyagi, L. Tomar, Y.E. Choonara, L.C. du Toit, P. Kumar, C. Penny and V. Pillay, *Int. J. Nanomedicine*, **9**, 589 (2014); https://doi.org/10.2147/IJN.S50941
2. P.P.N. Kumar, U. Shameem, P. Kollu, R.L. Kalyani and S.V.N. Pammi, *Bionanoscience*, **5**, 135 (2015); https://doi.org/10.1007/s12668-015-0171-z
3. Y. Wang, F.-A. Khan, M. Siddiqui, M. Aamer, C. Lu, Atta-Ur-Rahman, Atia-Tul-Wahab and M.I. Choudhary, *J. Ethnopharmacol.*, **279**, 113675 (2021); https://doi.org/10.1016/j.jep.2020.113675
4. S. Banerjee, A. Das, P. Chakraborty, K. Suthindhiran and M.A. Jayasri, *Pak. J. Biol. Sci.*, **17**, 715 (2014); https://doi.org/10.3923/pjbs.2014.715.719
5. Y. Shi, D. Pu, X. Zhou and Y. Zhang, *Foods*, **11**, 3408 (2022); https://doi.org/10.3390/foods11213408
6. M.V. Hormaiztegui, M.I. Aranguren and V.L. Mucci, *Eur. Polym. J.*, **102**, 151 (2018); https://doi.org/10.1016/j.eurpolymj.2018.03.020
7. E. Golestani, M. Javanbakht, H. Ghafarian-Zahmatkesh, H. Beydaghi and M. Ghaemi, *Electrochim. Acta*, **259**, 903 (2018); https://doi.org/10.1016/j.electacta.2017.10.123
8. S. Ören, T. Çaykara, Ö. Kantoglu and O. Güven, *J. Appl. Polym. Sci.*, **78**, 2219 (2000); https://doi.org/10.1002/1097-4628(20001213)78:12<2219::AID-APP200>3.0.CO;2-X
9. G. Chitra, D.S. Franklin, S. Sudarsan, M. Sakthivel and S. Guhanathan, *Int. J. Biol. Macromol.*, **95**, 363 (2017); https://doi.org/10.1016/j.ijbiomac.2016.11.068
10. X. Xu, J. Lin and P. Cen, *Chin. J. Chem. Eng.*, **14**, 419 (2006); https://doi.org/10.1016/S1004-9541(06)60094-3
11. T. Plisko, K. Burts, A. Penkova, M. Dmitrenko, A. Kuzminova, S. Ermakov and A. Bildyukevich, *Polymers*, **15**, 1664 (2023); https://doi.org/10.3390/polym15071664
12. K.K. Ajekwene, Properties and Applications of Acrylates, IntechOpen (2020).
13. J.E. Glass, *J. Coatings Technology*, **73**, 79 (2001); https://doi.org/10.1007/BF02698434
14. R. Brighenti, Y. Li and F.J. Vernerey, *Front. Mater.*, **7**, 196 (2020); https://doi.org/10.3389/fmats.2020.00196
15. E. Kostansek, *J. Coat. Technol. Res.*, **4**, 375 (2007); https://doi.org/10.1007/s11998-007-9037-9
16. R. Oliva, M.A. Ortenzi, A. Salvini, A. Papacchini and D. Giomi, *RSC Adv.*, **7**, 12054 (2017); https://doi.org/10.1039/C7RA00676D
17. S. Lin-Gibson, S. Bencherif, J.A. Cooper, S.J. Wetzel, J.M. Antonucci, B.M. Vogel, F. Horkay and N.R. Washburn, *Biomacromolecules*, **5**, 1280 (2004); https://doi.org/10.1021/bm0498777
18. R.S. Tomar, I. Gupta, R. Singhal and A.K. Nagpal, *Des. Monomers Polym.*, **10**, 49 (2007); https://doi.org/10.1163/156855507779763685
19. S. Fang, G. Wang, P. Li, R. Xing, S. Liu, Y. Qin, H. Yu, X. Chen and K. Li, *Int. J. Biol. Macromol.*, **115**, 754 (2018); https://doi.org/10.1016/j.ijbiomac.2018.04.072
20. D.S. Franklin and S. Guhanathan, *J. Appl. Polym. Sci.*, **132**, (2015); https://doi.org/10.1002/app.41921
21. S.J. Peighambardoust, S.H. Peighambardoust, N. Pournasir and P.M. Pakdel, *Food Packag. Shelf Life*, **22**, 100420 (2019); https://doi.org/10.1016/j.fpsl.2019.100420
22. S. Shankar, L.F. Wang and J.W. Rhim, *Carbohydr. Polym.*, **169**, 264 (2017); https://doi.org/10.1016/j.carbpol.2017.04.025
23. F. Zhang, Z. Xu, S. Dong, L. Feng, A. Song, C.H. Tung and J. Hao, *Soft Matter*, **10**, 4855 (2014); https://doi.org/10.1039/c4sm00479e
24. Z.Q. Zhu, H.X. Sun, X.J. Qin, L. Jiang, C.J. Pei, L. Wang, Y.Q. Zeng, S.H. Wen, P.Q. La, A. Li and W.Q. Deng, *J. Mater. Chem.*, **22**, 4811 (2012); https://doi.org/10.1039/c2jm14210d
25. Y. Ma, L. Lv, Y. Guo, Y. Fu, Q. Shao, T. Wu, S. Guo, K. Sun, X. Guo, E.K. Wujcik and Z. Guo, *Polymer*, **128**, 12 (2017); https://doi.org/10.1016/j.polymer.2017.09.009
26. Y. Huang, M. Zeng, J. Ren, J. Wang, L. Fan and Q. Xu, *Colloids Surf. A Physicochem. Eng. Asp.*, **401**, 97 (2012); https://doi.org/10.1016/j.colsurfa.2012.03.031
27. G. Kowalski, K. Kijowska, M. Witczak, L. Kuterasiñski and M. Lukasiewicz, *Polymers*, **11**, 114 (2019); https://doi.org/10.3390/polym11010114
28. A. Altinisik and K. Yurdakoc, *J. Appl. Polym. Sci.*, **122**, 1556 (2011); https://doi.org/10.1002/app.34278
29. K. Ghanbari and Z. Babaei, *Anal. Biochem.*, **498**, 37 (2016); https://doi.org/10.1016/j.ab.2016.01.006
30. A. Lavin, R. Sivasamy, E. Mosquera and M.J. Morel, *Surf. Interfaces*, **17**, 100367 (2019); https://doi.org/10.1016/j.surfin.2019.100367
31. S. Gandhi, R.H.H. Subramani, T. Ramakrishnan, A. Sivabalan, M.G. Nair, V. Dhanalakshmi and R. Anbarasan, *J. Mater. Sci.*, **45**, 1688 (2010); https://doi.org/10.1007/s10853-009-4158-4
32. Z. Zhou, C. Lu, X. Wu and X. Zhang, *RSC Adv.*, **3**, 26066 (2013); https://doi.org/10.1039/c3ra43006e
33. M. Yadollahi, I. Gholamali, H. Namazi and M. Aghazadeh, *Int. J. Biol. Macromol.*, **73**, 109 (2015); https://doi.org/10.1016/j.ijbiomac.2014.10.063
34. R.J. Pinto, S. Daina, P. Sadocco, C.P. Neto and T. Trindade, *BioMed Res. Int.*, **2013**, 280512 (2013); https://doi.org/10.1155/2013/280512